Transport in Porous Media (2005) 61:1–14
DOI 10.1007/s11242-004-2556-2

Vortex Instability of the Asymptotic Dissipation Profile in a Porous Medium

D. A. S. REES[1], E. MAGYARI[2] and B. KELLER[2]
[1]*Department of Mechanical Engineering, University of Bath, Bath, BA2 7AY, UK*
[2]*Chair of Physics of Buildings, Institute of Building Technology, Swiss Federal Institute of Technology (ETH), Zürich, Wolfgang-Pauli-Street 1, HIL E, CH-8093 Zürich, Switzerland*

(Received: 14 October 2003; accepted in final form: 26 August 2004)

Abstract. In this note we consider the thermoconvective stability of the recently-discovered asymptotic dissipation profile (ADP). The ADP is a uniform thickness, parallel-flow boundary layer which is induced by a cold surface in a warm saturated porous medium in the presence of viscous dissipation. We have considered destabilisation in the form of stream-wise vortex disturbances. The critical wavenumber and Rayleigh number for the onset of convection have been determined for all angles of the cooled surface between the horizontal and the vertical for which the ADP exists. The paper closes with a presentation of some strongly nonlinear computations of steady vortices.

Key words: free convection, porous media, boundary-layer, viscous dissipation, vortex instability.

1. Introduction

In the last few years there has been much interest in how the presence of viscous dissipation affects free, mixed and forced convective flows in porous media. The first published works showing that the rate of heat generation by viscous dissipation in porous media is proportional to the square of the seepage speed are those by Ene and Sanchez-Palencia (1982) and Bejan (1995). Nakayama and Pop (1989) were then the first to apply this model to a thermal boundary layer flow while Ingham *et al.* (1990) applied it to mixed convection in a uniform channel. All of these papers assume that the momentum equation is given by Darcy's law; the modelling of viscous dissipation uses further terms when form-drag and boundary effects are significant (see Rees *et al.*, 2005).

An important property of viscous dissipation in porous media is that it removes up/down symmetry from certain fluid flows. For example, when viscous dissipation is negligible, then the flow induced by a constant temperature heated surface which is projecting upwards is mathematically identical to that induced by a similar downward-projecting cold surface. This symmetry no longer exists when viscous dissipation is present, since, for the hot

surface, the heat generated serves to accelerate the flow, while, for the cold surface buoyancy, is retarded. In the latter case Magyari and Keller (2003) showed that a uniform thickness boundary layer with parallel flow is a possible solution of the governing equations, and it decays algebraically rather than exponentially. A little later Rees *et al*. (2003) showed that this flow is achievable in practice, at least within the confines of the boundary layer approximation. Rees *et al*. (2003) showed that the flow near the leading edge is identical to that obtained by Cheng and Minkowycz (1977), but that the usual unbounded growth of the boundary layer thickness with distance from the leading edge is restrained by the presence of viscous dissipation, and the boundary layer tends towards the parallel-flow solution of Magyari and Keller (2003). Therefore the solution of Magyari and Keller (2003) has been named the asymptotic dissipation profile (ADP) due to its similarity to the asymptotic suction profile which has the same qualitative features.

The aim of the present paper is to consider the stability of the ADP which forms on generally inclined cold surfaces which are downward facing. It is essential to do this, for should the ADP be found to be unstable, then any flow patterns and heat transfer correlations deriving from the ADP will be incorrect in practice. The basic flow is identical to that of the vertical ADP of Magyari and Keller (2003) except that its thickness depends on the inclination of the cooled surface. This solution is perturbed by small-amplitude vortex disturbances of wavenumber k, and the value of critical Rayleigh is determined as a function of k. The stability analysis is then extended into the nonlinear regime with some fully numerical computations of the vortex system using a suitable finite difference method. The evolution of the shape of the vortices with increasing Rayleigh number is shown.

2. Equations of Motion and Basic Flow

Convection is induced by the presence of a cold surface embedded within an otherwise hot porous medium. We assume that the flow is governed by Darcy's law modified by the presence of buoyancy and subject to the Boussinesq approximation. In writing the energy equation it is further assumed that the fluid and the porous matrix are in local thermal equilibrium, and that viscous dissipation is significant. Thus we use the following equations:

$$\frac{\partial \bar{u}}{\partial \bar{x}} + \frac{\partial \bar{v}}{\partial \bar{y}} + \frac{\partial \bar{w}}{\partial \bar{z}} = 0, \tag{1}$$

$$\bar{u} = -\frac{K}{\mu}\frac{\partial \bar{p}}{\partial \bar{x}} - \frac{\rho g \beta K (T - T_\infty)}{\mu}\cos\alpha, \tag{2}$$

$$\bar{v} = -\frac{K}{\mu}\frac{\partial \bar{p}}{\partial \bar{y}} - \frac{\rho g \beta K (T - T_\infty)}{\mu} \sin \alpha, \tag{3}$$

$$\bar{w} = -\frac{K}{\mu}\frac{\partial \bar{p}}{\partial \bar{z}}, \tag{4}$$

$$\sigma \frac{\partial T}{\partial \bar{t}} + \bar{u}\frac{\partial T}{\partial \bar{x}} + \bar{v}\frac{\partial T}{\partial \bar{y}} + \bar{w}\frac{\partial T}{\partial \bar{z}} = \kappa \left(\frac{\partial^2 T}{\partial \bar{x}^2} + \frac{\partial^2 T}{\partial \bar{y}^2} + \frac{\partial^2 T}{\partial \bar{z}^2} \right) + \frac{\nu}{K c_p} \left(\bar{u}^2 + \bar{v}^2 + \bar{w}^2 \right), \tag{5}$$

see Nield and Bejan (1999). In these equations $\bar{x}$, $\bar{y}$ and $\bar{z}$ are the streamwise, cross-stream and spanwise coordinates, respectively, and the corresponding seepage velocities are $\bar{u}$, $\bar{v}$ and $\bar{w}$. All other terms have their usual meaning in the context of porous media: K is the permeability, σ is the heat capacity ratio of the porous medium to that of the fluid, μ is the dynamic viscosity, $\nu = \mu/\rho$ is the kinematic viscosity, where ρ is the reference density of the fluid, i.e. when the temperature is given by $T = T_\infty$. The cold surface is held at the temperature T_w, where $T_w < T_\infty$. Finally the quantities g, β, κ and c_p are gravity, the coefficient of cubical expansion, the inclination of the cold surface away from the downward vertical and specific heat, respectively. The flow configuration is sketched in Figure 1, where the $\bar{z}$-direction is perpendicular to the diagram.

Equations (1)–(5) are nondimensionalised using the following scalings:

$$T = T_\infty + (T_w - T_\infty)\theta, \qquad \bar{x} = Lx, \qquad (\bar{y}, \bar{z}) = LR^{-1/2}(y, z),$$
$$\bar{t} = \frac{\sigma L^2}{\kappa R} t, \qquad \bar{u} = \frac{\kappa R}{L} u, \qquad (\bar{v}, \bar{w}) = \frac{\kappa R^{1/2}}{L}(v, w), \qquad \bar{p} = \frac{\mu \kappa R^{1/2}}{K} p. \tag{6}$$

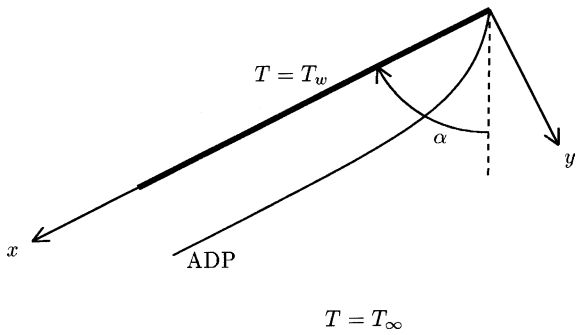

Figure 1. A sketch of the flow domain indicating the axes, the orientation of the cold surface (thick line) relative to the downward vertical, and a depiction of the development of the boundary layer towards the ADP.

The length scale L used in (6) arises naturally in the system due to the presence of viscous dissipation and is given by

$$L = \frac{c_p}{g\beta}. \tag{7}$$

The value R is the Darcy–Rayleigh number defined by

$$R = \frac{\rho g \beta K (T_\infty - T_w) L}{\mu \kappa}. \tag{8}$$

These scalings were devised by Rees *et al.* (2003) when considering the development of the ADP at high values of R, and it was found that the boundary layer thickness is of $O(LR^{-1/2})$ while the entry length for the boundary layer itself is of $O(L)$; this is the motivation behind the different scaling for $\bar{x}$ and for $\bar{y}$ and $\bar{z}$. Consequently $\bar{u}$ must be scaled differently from $\bar{v}$ and $\bar{w}$.

The governing equations now reduce to the form

$$\frac{\partial u}{\partial x} + \frac{\partial v}{\partial y} + \frac{\partial w}{\partial z} = 0, \tag{9}$$

$$u = -R^{-1/2} \frac{\partial p}{\partial x} + \theta \cos \alpha, \tag{10}$$

$$R^{-1/2} v = -\frac{\partial p}{\partial y} + \theta \sin \alpha, \tag{11}$$

$$R^{-1/2} w = -\frac{\partial p}{\partial z}, \tag{12}$$

$$\frac{\partial \theta}{\partial t} + u\frac{\partial \theta}{\partial x} + v\frac{\partial \theta}{\partial y} + w\frac{\partial \theta}{\partial z} = R^{-1}\frac{\partial^2 \theta}{\partial x^2} + \frac{\partial^2 \theta}{\partial y^2} + \frac{\partial^2 \theta}{\partial z^2} - u^2 - R^{-1}(v^2 + w^2), \tag{13}$$

while the boundary conditions are that

$$y = 0: \quad v = 0, \quad \theta = 1, \tag{14}$$

$$y \to \infty: \quad u, \theta \to 0. \tag{15}$$

In this paper we are not assuming that $R \gg 1$ and therefore that the boundary layer approximation is valid, rather, we are taking R to be finite, but assume that x is sufficiently large that a uniform thickness x-independent flow has been attained.

The basic flow we analyse for stability is a constant thickness boundary layer where all flow quantities are steady and independent of x, the streamwise direction, as found by Magyari and Keller (2003). The sole difference between the present problem and that of Magyari and Keller (2003) is that the cold surface is inclined away from vertical in the manner depicted in

Figure 1. In this situation we will assume both x- and z-independence and therefore (9) implies that $u = u(y)$. Equations (10) and (13) become

$$u = \theta \cos\alpha, \qquad \frac{\partial^2 \theta}{\partial y^2} - u^2 = 0. \tag{16, 17}$$

The solution for θ is

$$\theta = \frac{6}{(y \cos\alpha + \sqrt{6})^2}, \tag{18}$$

which is an algebraically decaying solution. We note that the thickness of the boundary layer increases as α increases from zero. It proves very convenient to have a description of the basic flow which is independent of $\cos\alpha$, and therefore we define the variables, $\hat{y}$ and $\hat{z}$ according to

$$\hat{y} = y \cos\alpha, \qquad \hat{z} = z \cos\alpha. \tag{19}$$

We denote the basic solution in the following way:

$$u_b = F(\hat{y}) \cos\alpha, \qquad v_b = w_b = p_b = 0, \qquad \theta_b = F(\hat{y}), \tag{20}$$

where

$$F(\hat{y}) = \frac{6}{(\hat{y} + \sqrt{6})^2}. \tag{21}$$

3. Stability Analysis

Equations (9)–(13) may now be transformed according to (19) and linearised about the solution given in (20) using

$$(u, v, w, p, \theta) = (u_b, v_b, w_b, p_b, \theta_b) + (U, V, W, P, \Theta), \tag{22}$$

where the quantities, U, V, W, P and Θ, are assumed to be infinitesimally small. We will be taking disturbances of the form of streamwise vortices whose form is independent of x, since this is a parallel basic flow. We also invoke the principle of exchange of stabilities, which may be proved for this system, and which allows us to set the time-derivative term in (13) to zero.

After all these operations, the linearised stability equations become

$$\frac{\partial V}{\partial \hat{y}} + \frac{\partial W}{\partial \hat{z}} = 0, \tag{23}$$

$$U = \Theta \cos \alpha, \tag{24}$$

$$R^{-1/2} V = -\frac{\partial P}{\partial \hat{y}} cos\, \alpha + \Theta \sin \alpha, \tag{25}$$

$$R^{-1/2} W = -\frac{\partial P}{\partial \hat{z}} cos\, \alpha, \tag{26}$$

$$(F' \cos \alpha) V + (2F \cos \alpha) U = \frac{\partial^2 \Theta}{\partial \hat{y}^2} + \frac{\partial^2 \Theta}{\partial \hat{z}^2}, \tag{27}$$

and they may be simplified by substituting for U from Equation (24) into Equation (27), and by introducing the streamfunction, Ψ, according to

$$V = \frac{\partial \Psi}{\partial \hat{y}} \cos \alpha, \qquad W = -\frac{\partial \Psi}{\partial \hat{z}} \cos \alpha. \tag{28}$$

The linearised stability equations now become

$$\frac{\partial^2 \Psi}{\partial \hat{y}^2} + \frac{\partial^2 \Psi}{\partial \hat{z}^2} = R^{1/2} \tan \alpha \frac{\partial \Theta}{\partial \hat{z}} \tag{29}$$

$$\frac{\partial^2 \Theta}{\partial \hat{y}^2} + \frac{\partial^2 \Theta}{\partial \hat{z}^2} - 2F(y)\Theta = F'(\hat{y}) \frac{\partial \Psi}{\partial \hat{z}}. \tag{30}$$

Vortices may be introduced by setting

$$\Psi = f(\hat{y}) \cos k\hat{z}, \qquad \Theta = g(\hat{y}) \sin k\hat{z}, \tag{31, 32}$$

and we obtain the following ordinary differential eigenvalue problem for f and g:

$$f'' - k^2 f = (R^{1/2} \tan \alpha) kg, \qquad g'' - (k^2 + 2F) g = -F' kf, \tag{33, 34}$$

which must be solved subject to the boundary conditions

$$f = g = 0 \quad \text{at} \quad \hat{y} = 0 \quad \text{and} \quad f, g \to 0 \quad \text{as} \quad \hat{y} \to \infty. \tag{35}$$

These equations were solved using the classical 4th order Runge–Kutta method combined with a standard multidimensional shooting method to find the variation of the eigenvalue, $R^{1/2} \tan \alpha$ with the vortex wavenumber, k. Thus it is essential to force nonzero solutions by imposing the further boundary condition

$$g'(0) = 1. \tag{36}$$

Numerical solutions were obtained using a steplength of 0.1 in the $\hat{y}$-direction; this is sufficiently small to yield excellent accuracy using a fourth order method. We also note that, despite the basic solution exhibiting algebraic decay, the disturbances which form the solution to (33) and (34) decay exponentially. The maximum value of $\hat{y}$ which was used varies between 7 when k is relatively large and 200 when k is small.

Figure 2 shows how the critical value of $R^{1/2}\tan\alpha$ varies with wavenumber, k. Not surprisingly the neutral curve follows the standard Bénard-like behaviour of having a single well-defined minimum and of rising towards infinity as $k \to 0$ and $k \to \infty$. The interpretation of the curve is also the usual one, namely, that points above the curve correspond to growing vortex disturbances, while decaying disturbances are represented by points below the curve.

It is important to determine the minimum value of $\mathrm{R}^{1/2}\tan\alpha$ since this yields a global linear stability criterion in a spanwise-unbounded layer. This was achieved by adding to Equations (33) and (34) a system formed by differentiating (33) and (34) with respect to k, and by taking $\partial(R^{1/2}\tan\alpha)/\partial k = 0$. The resulting system yields the following result:

$$k_c = 0.5166, \quad (R^{1/2}\tan\alpha)_c = 16.8469, \tag{37}$$

which are correct to the quoted number of places.

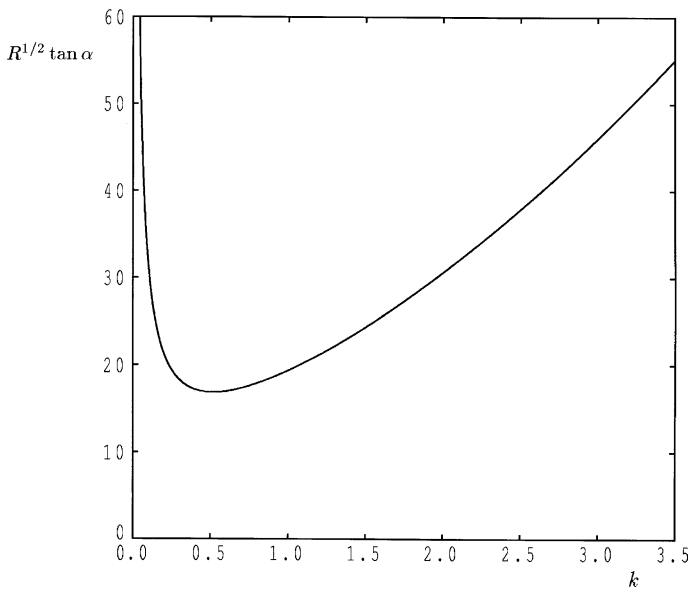

Figure 2. The neutral curve for the onset of vortex convection in the asymptotic dissipation profile. Profits above the curve represent unstable disturbances. the minimum lies at $k = 0.5166$ and $R^{1/2}\tan\alpha = 16.8469$.

The critical wavenumber may be compared with π, which corresponds to the critical wavenumber in the classical Darcy–Bénard problem which comprises a layer of uniform thickness (equal to unity). In the present flow the thickness of the boundary layer is substantially greater than 1, therefore the thickness (see Figure 3) and wavelength of the vortex will also be greater than 1, and this corresponds to a much smaller critical wavenumber than π.

The critical value of R is strongly dependent on the value of α. When $\alpha \to 0^+$ then the critical Rayleigh number increases without bound, and we conclude that the vertical ADP is stable. This situation is similar to that for free convective flow in a vertical channel subject to a horizontal temperature gradient, and which was proved by Gill (1969) to be stable using an energy stability method. It is also similar to the classical vertical thermal boundary layer flow from a uniformly hot surface in a porous medium; see Lewis *et al.* (1995) and Rees (1993).

The flow is also stable when α is negative, for this corresponds to a cold surface lying below a warm region. Finally, as $\alpha \to 1/2\pi$, the horizontal limit, the critical Rayleigh number tends towards zero. In fact, this is not an achievable limit within the current analyses since the boundary layer has become infinitely thick.

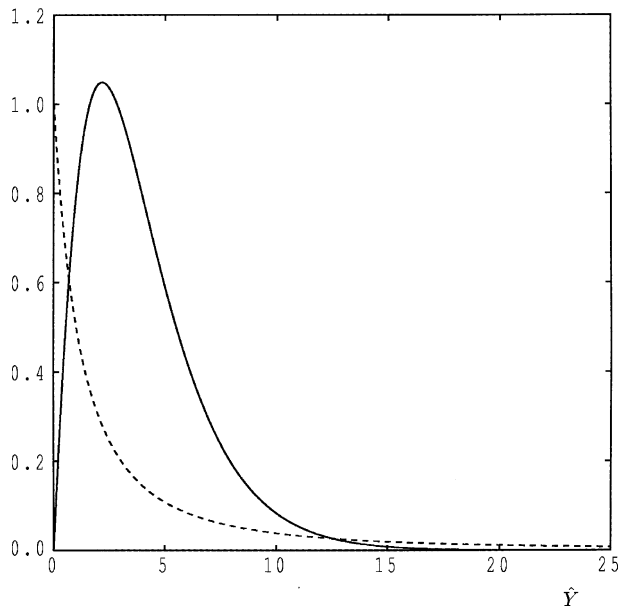

Figure 3. The variation with $\hat{y}$ of (i) $g(\hat{y})$. the temperature perturbation (continuous curve); and (ii) $F(\hat{y})$, the basic temperature profile (dashed curve). The disturbance was computed at the critical value of $k : k_c = 0.5166$.

4. Nonlinear Vortices

In this brief section we present some preliminary computations of nonlinear vortices which arise at Rayleigh numbers higher than those given by Equation (37). The full nonlinear equations are

$$\frac{\partial^2\Psi}{\partial\hat{y}^2}+\frac{\partial^2\Psi}{\partial\hat{z}^2}=R^{1/2}\tan\alpha\frac{\partial\Theta}{\partial\hat{z}} \tag{38}$$

$$\frac{\partial^2\Theta}{\partial\hat{y}^2}+\frac{\partial^2\Theta}{\partial\hat{z}^2}-2F\Theta-F'\frac{\partial\Psi}{\partial\hat{z}}=\frac{\partial\Psi}{\partial\hat{z}}\frac{\partial\Theta}{\partial\hat{y}}-\frac{\partial\Psi}{\partial\hat{y}}\frac{\partial\Theta}{\partial\hat{z}}+\Theta^2 +R^{-1}\left[\left(\frac{\partial\Psi}{\partial\hat{y}}\right)^2+\left(\frac{\partial\Psi}{\partial\hat{z}}\right)^2\right]+\frac{\partial\Theta}{\partial t}, \tag{39}$$

which are to be solved subject to the boundary conditions that both Ψ and Θ are zero on $\hat{y}=0$ and become zero as $\hat{y}\to\infty$. In Equations (38) and (39) both Ψ and Θ are $O(1)$ quantities and they represent the full nonlinear perturbation to the steady ADP. In the computations presented below we assumed that the cooled surface is at an angle $\pi/4$ to the vertical and we have considered a selection of values of R in order to see how the vortices change when R increases.

The numerical method chosen was modified from the code developed by Rees and Bassom (1993) and is a fully implicit scheme based on second order accurate central differences in space and a first order accurate backward difference scheme in time. The Jacobian term was modelled using the well-known Arakawa (1966) formula. Computations proceeded by seeding a suitable disturbance and following it to the steady-state. The advantage of using a fully implicit scheme is that the steady-state solution is achieved in much less CPU time than by using other explicit or pseudo explicit methods such as the forward difference or DuFort Frankel methods. A DuFort Frankel time-stepping code was also developed and the results compared very favourably with those of the backward difference scheme, although the timestep had then to be restricted to near 0.01 in order to maintain numerical stability.

We chose a computational domain of 48 points in the $\hat{z}$-direction and 96 in the $\hat{y}$-direction. In terms of spatial variables the computational domain was $0\leqslant\hat{z}\leqslant 12$ and $0\leqslant\hat{y}\leqslant 24$. The former range is equivalent to the wavenumber $k=0.5236$ which is very close to the critical value given in (37). The latter range was found to be sufficient to contain the vortex system. The grid aspect ratio is precisely unity, and therefore we used a pointwise (rather than line-wise) Gauss–Seidel method as the basic smoother. Iterative convergence was improved substantially by adopting a fully nonlinear multigrid method with V-cycling, as described in Brandt (1984) and as implemented in Rees and Bassom (1993) and Rees (1993). Additionally, we

used a crude form of timestep control where the timestep was allowed to increase when the number of V-cycles was sufficiently small with a maximum timestep of 1 being imposed.

In general the computations were started using the relatively small timestep of 0.001, but this always increased gradually towards 1, our choice of maximum timestep, as the computation progressed. Convergence to the steady state was monitored by checking the size of largest absolute change in Θ in neighbouring timesteps, and convergence was deemed to have taken place when this change was less than 10^{-8}. This criterion, together with the large timesteps used towards the end of the computation yielded at least six figures of accuracy of the steady discretised system (as opposed to being compared with the precise solution).

Figure 4 shows the results of our computations for $R^{1/2} = 17$, 18, 20, 25, 30 and 40 where the cooled surface is inclined at an angle of $\alpha = 45^\circ$. In this figure are displayed the streamlines and both the perturbation and full temperature fields. The streamlines shown in the top row of Figure 4 indicate the manner in which fluid particles move in the $y - z$ plane. The streamwise motion, which is perpendicular to that plane, is $u_b + U$: see Equation (22). The definition of u_b is given by (20) and U by Equation (24). The superimposition of these two motions yields particle paths which are helical.

When $R^{1/2} = 17$ conditions are only just post-critical, and there are only slight deviations in the isotherms away from the straight lines corresponding to the ADP. The streamlines also display a left / right symmetry about their maxima and minima, which is consistent with the substitutions (31) and (32). When the value of R increases, the strength of the vortices increases and the boundary layer becomes thicker. The symmetry alluded to above is lost due to the fact that the flow away from the cooled surface takes place into an unbounded region, while inflow in constrained by the presence of the surface. In fact we see the gradual development of a strong jet of cold fluid away from the surface as R increases, and this increasing strength accounts for the increase in the boundary layer thickness. The shape of the perturbation isotherms alters quite markedly with the development of a very distinctive triangular-shaped region of relatively warm fluid, while the cold regions grow outwards and begin to join together some distance from the cooled surface.

Given that viscous dissipation is present, the vortex flow gives an additional dissipative effect which will raise the mean temperature of the porous medium near the cooled surface. As a simple means of assessing the magnitude of this effect, we have integrated the perturbation temperature field, Θ, over the whole computational domain using a straightforward two-dimensional form of the trapezium rule. The results of this computation are shown in Table I and we denote the mean temperature as Θ_{m}.

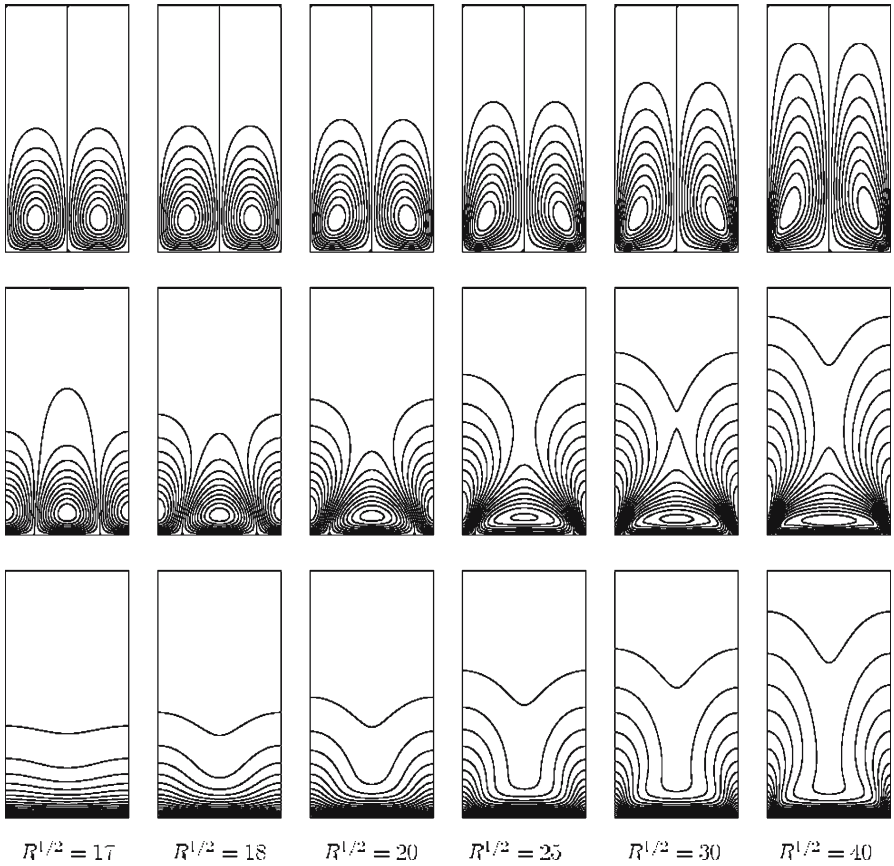

Figure 4. Streamlines (top row), perturbation isotherms (middle row) and isotherms (bottom row) for nonlinear vortices within the ADP for a cold surface at 45° to the vertical, for a range of values of R. The vertical coordinate in these contour plots is $\hat{y}$, and horizontal cordinate is $\hat{z}$.

We note that Θ_m is usually zero for Darcy-Bénard-like problems since such flows retain the symmetry between positive and negative perturbations, but here the viscous dissipative effect removes the symmetry. We find that Θ_m increases with R indicating that there is, not surprisingly, an extra heating effect on the fluid. It is also of interest to note that a linear extrapolation of the data for $R^{1/2} = 17$ and 18 to determine, where Θ_m returns to zero, which marks the onset of convection, shows that $R^{1/2} = 16.904$, a value which is in error by 0.34% compared with the value given in (37).

In further computations at inclinations which are closer to the vertical, the computed flows are similar to those presented here because the coefficient of $(\Psi_{\hat{y}}^2 + \Psi_{\hat{z}}^2)$ in (39) is very small. However, we have found some

Table I. Variation of Θ_m with $R^{1/2}$

$R^{1/2}$	Θ_m
17	0.000269
18	0.003084
20	0.008253
25	0.019403
30	0.029067
35	0.037308
40	0.044408

qualitative differences when α corresponds to inclinations which are closer to the horizontal. In some cases it is possible for this vortex system to become destabilised and form four vortices instead of the original two. It appears, therefore, that the postcritical development deserves a much more comprehensive treatment than may be given here, and we intend to report on it in the future.

5. Conclusions

In this paper we have determined the stability characteristics for the ADP induced by a generally inclined cold surface embedded in a warm porous medium in the presence of viscous dissipation. It has been shown that the ADP is stable when the cooled surface is vertical. At inclinations lying between the vertical ($\alpha = 0$) and the horizontal ($\alpha = \pi/2$) the critical value of the Rayleigh number is given by $R_c = (16.8469 \cot \alpha)^2$, and is therefore a decreasing function of α in this range. The critical wavelength is $2\pi/0.5166 \cos \alpha$, in terms of the original nondimenional coordinate, z, and this increases in direct proportion to the thickness of the ADP itself.

At postcritical Rayleigh numbers nonlinear vortices occur and these have been found to increase the thickness of the boundary layer as R increases. Strong outflow jets were also found to grow with increasing R, and the presence of more intense flow also serves to increase the mean temperature of the boundary layer.

Appendix

For a porous region composed of a sand with water as the saturating fluid, we may take the following as typical values. For sand we have Density: $\rho = 2000\,\mathrm{kg/m^3}$; specific heat: $c_p = 800\,\mathrm{J/kg\ K}$; permeability: $K = 10^{-10}\,\mathrm{m^2}$. For water we have diffusivity: $\kappa = 1.44 \times 10^{-7}\mathrm{m^2/s}$; dynamic viscosity: $\mu = 0.001\,\mathrm{kg/ms}$; coefficient of cubical expansion: $\beta = 4 \times 10^{-4}\,\mathrm{K^{-1}}$. Finally we may assume a temperature variation of 50 K.

From (6) we see that the dimensional lengthscale corresponding to the boundary layer thickness has magnitude $L/R^{1/2}$, where L is defined in Equation (7) and R in Equation (8). Therefore we obtain the value

$$L/R^{1/2} = \left(\frac{\mu \kappa c_p}{\rho (g\beta)^2 K (T_\infty - T_w)} \right)^{1/2} \simeq 27.4\,\mathrm{m}. \tag{A.1}$$

Given that the thermal boundary layer whose stability is being analysed has thickness roughly equal to 5 in nondimensional terms, this means that the boundary layer has dimensional thickness of the order of $(140/\cos\alpha)$m. Therefore the ADP is most likely to arise in geologically sized regions, and is unlikely to be achievable in laboratory experiments.

References

Arakawa, A.: 1966, Computational design of long-term numerical integration of the equations of fluid motion: I. Two-dimensional incompressible flow, *J. Comp. Phys*. **1**, 119–143.

Bejan, A.: 1995, *Convection Heat Transfer (2nd Edition)*, John Wiley & Sons, New York.

Brandt, A.: 1984, Multigrid techniques: 1984 guide with applications to fluid dynamics. *Lecture notes in C.F.D*. at the Von Karman Institute for Fluid Dynamics. Published by G.M.D. mbH, Bonn as *GMD–Studien* **85**.

Cheng, P. and Minkowycz, W. J.: 1977, Free convection about a vertical flat plate embedded in a porous medium with application to heat transfer from a dike, *J. Geophys. Res*. **82**, 2040–2044.

Ene, H. I. and Sanchez-Palencia, E.: 1982, On thermal equation for flow in porous media, *Int. J. Eng. Sci*. **20**, 623–630.

Gill A. E.: 1969, A proof that convection in a porous vertical slab is stable, *J. Fluid Mech*. **35**, 545–547.

Ingham, D. B., Pop, I. and Cheng, P.: 1990, Combined free and forced convection in a porous medium between two vertical walls with viscous dissipation, *Transp. Porous Media* **5**, 381–398.

Lewis, S. Bassom, A. P. and Rees, D. A. S.: 1995, The stability of vertical thermal boundary layer flow in porous medium, *Eur. J. Mech. B: Fluids* **14**, 395–408.

Magyari, E. and Keller, B.: 2003, The opposing effect of viscous dissipation allows for a parallel free convection boundary-layer along a cold vertical flat plate, *Trans. Porous Media* **51**, 227–230.

Nakayama, A. and Pop, I.: 1989, Free convection over a non-isothermal body in a porous medium with viscous dissipation, *Int. Comm. Heat Mass Transfer* **16**, 173–180.

Nield, D. A. and Bejan, A.: 1999, *Convection in Porous Media (2nd edition)*, Springer, New York.

Rees, D. A. S.: 1993, Nonlinear wave stability of vertical thermal boundary layer flow in a porous medium, *J. Appl. Math. Phy. (Z.A.M.P.)* **44**, 306–313.

Rees, D. A. S. and Bassom, A. P.: 1993, The nonlinear nonparallel wave instability of free convection induced by a horizontal heated surface in fluid-saturated porous media, *J. Fluid Mech.* **253**, 267–296.

Rees, D. A. S.: Magyari, E. and Keller, B.: 2003, The development of the asymptotic viscous dissipation profile in a vertical free convective boundary layer in a porous medium, *Transp. Porous Media* **53**, 347–355.

Rees, D. A. S., Magyari, E. and Keller, B.: 2005, 'Effect of viscous dissipation on the flow in fluid saturated porous media' in K. Vafai, (Ed.), *Handbook of Porous Media II* Marcell-Dekker, New York.